Superconductivity in Bi 2223 compound: physics and potential applications

Babić, Emil; Kušević, Ivica; Zadro, Krešo; Ivkov, Jovica; Marohnić, Željko; Drobac, Đuro; Prester, Mladen; Liu, Hua Kun; Dou, Shi Xue; Todorović-Marinić, Dragana; ...

Source / Izvornik: **Fizika A, 1995, 4, 549 - 560**

Journal article, Published version
Rad u časopisu, Objavljena verzija rada (izdavačev PDF)

Permanent link / Trajna poveznica: https://urn.nsk.hr/urn:nbn:hr:217:551330

Rights / Prava: In copyright / Zaštićeno autorskim pravom.

Download date / Datum preuzimanja: **2024-04-20**

Repository / Repozitorij:

Repository of the Faculty of Science - University of Zagreb

ISSN 1330–0008
CODEN FIZAE4

SUPERCONDUCTIVITY IN Bi 2223 COMPOUND: PHYSICS AND POTENTIAL APPLICATIONS

EMIL BABIĆ[a], IVICA KUŠEVIĆ[a], KREŠO ZADRO[a], JOVICA IVKOV[b], ŽELJKO MAROHNIĆ[b], ĐURO DROBAC[b], MLADEN PRESTER[b], HUA KUN LIU[c], SHI XUE DOU[c], DRAGANA TODOROVIĆ–MARINIĆ[d] and AHMED KURŠUMOVIĆ[d]

[a] *Department of Physics, Faculty of Science, The University of Zagreb, POBox 162, 10001 Zagreb, Croatia*
[b] *Institute of Physics of the University, POBox 304, 10001 Zagreb, Croatia*
[c] *Centre for Superconducting and Electronic Materials, University of Wollongong, Wollongong, NSW 2522, Australia*
[d] *CIRM-Energoinvest, Sarajevo, Bosnia and Hercegovina*

Dedicated to Professor Mladen Paić on the occasion of his 90$^{\text{th}}$ birthday

Received 16 June 1995

UDC 538.945

PACS 74.72.-h, 74.72.Hs, 74.60.Ec, 74.60.Ge

The main results of the systematic study of the electron transport properties and AC susceptibility in Pb-doped, almost single phase, Bi 2223 ceramic samples and Ag-clad Bi 2223 tape, are presented. Whereas the results for the ceramic samples can only be used for the study of the percolation problem in the weak–link network, those for tape can yield some intrinsic parameters of Bi 2223 compound (the upper critical fields B_{C2}, the coherence lengths, etc.). In addition, the results for the tape provide some technologically relevant parameters (the pinning potential U_0, volume pinning force F_p and the flux-flow viscosity η) and an insight into the nature of dissipation and pinning in these materials. Some factors limiting the critical current density J_c in the present-day tapes are briefly discussed.

1. Introduction

$Bi_2Sr_2Ca_2Cu_3O_{10+y}$ (hereafter Bi 2223) compound is the first discovered high temperature superconductor (HTS) with the superconducting transition temperature, T_c, above 100 K. Within two months after the discovery of superconductivity in Bi-Sr-Ca-Cu-O compounds [1] the samples with the majority Bi 2223 phase were prepared and characterised at the Institute of Physics of the University in Zagreb.

Although Bi 2223 is among the eldest HTS, its properties are less known than those of any other HTS discovered until now. The reason is a lack of good quality single crystals caused by the decomposition of the Bi 2223 phase well below the melting temperature of the appropriate mixture of the constituents [2]. Even the fabrication of a single-phase Bi 2223 ceramic material proved to be very difficult. This is due to the slow reaction kinetics involved with the very narrow temperature window for formation of this phase in air [2]. As a result, no bulk Bi 2223 sample without a substantial amount ($\geq 20\%$) of $Bi_2Sr_2CaCu_2O_{8+x}$ (Bi 2212) and $Bi_2Sr_2Cu_1O_{6+z}$ (Bi 2201) phases has been obtained [3,4]. The thin film techniques appeared more efficient in preparing the almost single Bi 2223 phase. However the films [5,6] show some 10–30 K lower T_c than the bulk samples.

Doping with Pb proved to be beneficial in obtaining nearly pure Bi 2223 phase, both in bulk [2,7] and thin film samples [8]. Pb partially substitutes for Bi and widens the temperature window where the 2223 phase is formed [2]. Combined neutron and X-ray diffraction experiments on an almost single phase sample with composition $Bi_{1.89}Pb_{0.31}Sr_{2.0}Ca_{1.91}Cu_{3.0}O_{10+y}$ [9] indicated an A2aa crystal structure with the lattice parameters $a = 0.540$ nm, $b = 0.542$ nm and $c = 3.707$ nm. In comparison with the more familiar Bi 2212 structure [10], the 2223 phase features an additional CuO_2-Ca layer. The bulk (ceramic) Pb- doped Bi 2223 samples are almost useless for the study of intrinsic properties (other than crystalographic) of this compound. In particular, the random orientations of the crystalline axes of individual grains within the ceramic sample average out the effects of the anisotropy of Bi 2223 compound, which is essential for the understanding of its physical properties. Furthermore, in ceramic Bi 2223 samples the inevitable intergranular weak links (WL) mask efficiently the intrinsic behaviour of the homogeneous material [11]. Because of this, the early (limited) access to the intrinsic properties of the Bi 2223 compound was achieved via the study of the oriented Bi 2223 grains embeded in epoxy, the epitaxial films and small Pb-doped Bi 2223 whiskers [12].

The interest in Bi 2223 compound increased enormously upon the successful application of the powder-in-tube (PIT) technique for the production of Ag-clad Bi 2212 and 2223 wires and tapes [13]. This technique allowed the fabrication of large lengths (≥ 100 m) of dense, highly textured material, possesing high critical current density J_c. The reason for this is the micaceous structure of Bi 2212 and Bi 2223 compounds, which facilitates the alignment of grains within the tape [13]. This highly anisotropic structure makes the flux pinning in BSCCO compounds much weaker than in $YBa_2Cu_3O_{7-x}$ (YBCO) [14].

Here we present some novel results concerning the fundamental and application oriented properties of Pb-doped Bi 2223 compound. The results obtained from the

study of the electronic transport properties and AC susceptibility of an almost phase–pure high–J_c Ag–clad Bi 2223 tape will be compared with the literature data for the corresponding whisker [12], epitaxial films [6,15], other tapes [16] and with our previous (unpublished) results for the conventional Pb-doped Bi 2223 ceramic samples. The comparison shows that the intinsic properties deduced from the results for our tape are consistent with those for the corresponding whisker [12]. Finally, we shall briefly discuss some factors limiting J_c in the present-day Bi 2223 tapes and suggest some possible ways how to improve their critical currents. (J_c's).

2. Experimental

The details concerning the preparation of the investigated Ag-Bi 2223 tape were reported elsewhere [17]. A moderate annealing temperature and time resulted in a low fraction of the Bi 2212 phase ($\approx 2\%$), but also in rather small (≈ 10 mm) and, on average, not too well aligned grains. Furthermore, its core showed considerable porosity and some quite large impurity (nonsuperconducting) particles. As a result, when the intact tape of dimensions 15 mm × 4 mm × 0.12 mm was split along its length into two halves, they exhibited very different J_c's [18]. Here we discuss the results for a part of the tape having higher J_c only.

The methods employed for measurements of electrical resistivity ρ [18], J_c [17] and J_s (determined from the high resolution AC susceptibility [19]) have been previously described. The voltage criterion for the determination of J_c from the measured $V - I$ curves was few μV. All types of measurements were performed on the same samples. The resistivity was measured after J_c and J_s on a bare Bi 2223 core of the tape. The Ag-sheating was etched off using a solution of H_2O_2 and NH_4OH [18]. All measurements were made in the temperature (T) range 77–120 K and magnetic field $B \leq 1$ T. A special sample holder enabled rather accurate rotation ($\pm 1^\circ$) of the surface of the tape in respect to the field $\vec{B}$ direction. In all cases $\vec{B}$ was perpendicular to the current (J) direction.

The ceramic samples were prepared from the oxide and carbonate powders having the cation ratio Bi : Pb : Sr : Ca : Cu = 1.7 : 0.3 : 2.0 : 2.0 : 3.0. The powders were calcined at 820 °C for 10 h and the pellets (S_A) sintered at 850 °C for 240 h. Some pellets (S_B) were crushed into powder and resintered for 24 h at 850 °C. Pellets S_A showed large grains (≥ 20 mm) and low density (about 3 g/cm^3) whereas S_B had smaller grains (≤ 15 mm) and somewhat higher density (about 5 g/cm^3). The measurement techniques for these samples were the same as those for the tape. The actual measurements were performed on the rod–shaped samples (typical dimensions 15 mm ×15 mm ×1 mm), cut out from the pellets. The X-ray diffraction indicated low Bi 2212 content and no significant texture. Some data relevant to samples are given in Table 1.

3. Results and discussion

The resistivity measurements can yield the information about the fundamental properties of a given superconductor. However, for an anisotropic compound, quite large (about 1 mm) single crystals of a suitable shape are required for that purpose. Since for the Bi 2223 compound the good quality single crystals are not available,

one is compelled to use the whiskers [12] or tapes [20]. As mentioned before, since these materials are granular, one should take into account the possible effects of weak links and imperfect grain alignment when analysing the results.

TABLE 1.
Data relevant to Pb*-doped* Bi 2223 *tape and the corresponding ceramic sample* S_A : f *is the fraction of Bi 2212 phase,* ρ_n *is the resistivity at 120* K, B^c_{C2} *and* B^{ab}_{C2} *are the upper critical fields for* $B||c$ *and* $B \perp c$*, respectively,* ξ_{ab} *and* ξ_c *are the corresponding coherence lengths,* η *is the Bardeen–Stephen viscosity coefficient and* J_c *is the critical current density at* 77 K *in zero applied field.*

Sample	f (%)	ρ_n ($\mu\Omega$m)	B^c_{C2} (T)	B^{ab}_{C2} (T)	ξ_{ab} (nm)	ξ_c (nm)	η (μp)	J_c (kA/cm^2)
Tape	≈ 2	2.4	39	198	2.9	0.57	≈ 0.4	23
S_A	≈ 5	14						0.14

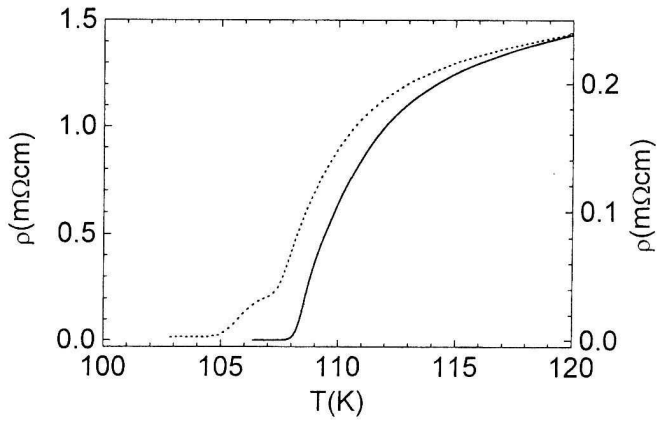

Fig. 1. Zero–field resistive transitions for a ceramic Bi 2223 *sample* S_A *(- - -, left scale) and the core of* Ag-Bi 2223 *tape (——, right scale).*

In Fig. 1, we compare the superconducting transitions ($B = 0$) for a core of our tape with that for the ceramic sample S_A. Whereas S_A shows a "foot" associated with the weak link system [11], the transition of the tape is smooth and is qualitatively the same as those for Bi 2223 epitaxial films [6] and whiskers [12]. Also, the normal state resistivity ρ_n for the core of our tape is sizeably lower than those for ceramic samples (Table 1), but is still up to a factor of two higher than ρ_n of the best Bi 2223 films [6,15] and whisker [12]. We believe that this enhanced ρ_n reflects the percolative current path within the tape (due to impurity particles, voids, tilt of the grains, "sausaging" of a core etc.) and not the contribution of the grain boundaries (weak links) to the resistance (as is the case in the ceramic samples [21]). The measurements of the differential (slope) resistance R_f for the same tape [22] support this conjecture. In particular, the observed very low R_f

($\approx 0.01R_n$), which increased with magnetic field B was consistent with the viscous flux–flow [22]. (In ceramic, samples R_f is associated with the resistance of the grain boundaries and is, therefore, practically independent of B and quite large ($\approx 0.1R_n$) for small grains [21].) The superconducting transitions studied by AC susceptibility for different amplitudes B_0 of the AC field are more sensitive test for the presence of the weak–link effects [11]. The single step transitions observed for all available values of B_0 indicated no observable weak link effects in our tape [19].

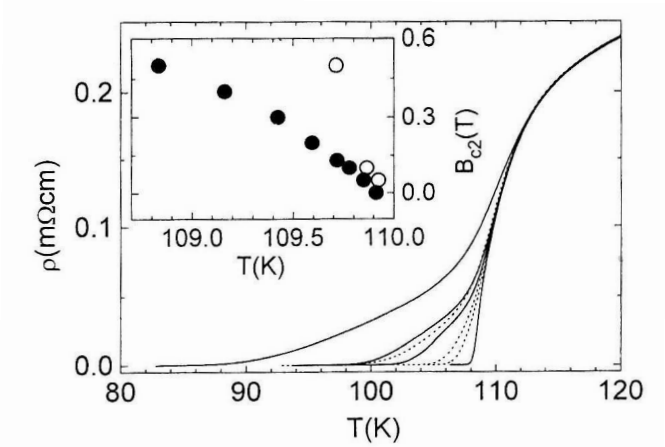

Fig. 2. Resistive transitions for the core of Ag-Bi 2223 *tape in field:* B = 0, 0.05, 0.1 and 0.5 T *(right to left) applied parallel (- - - -) and perpendicular (——-) to the plane of the tape. The inset: the plot of upper critical fields* B^c_{C2}(•) *and* B^{ab}_{C2} (○) *for the same tape versus temperature.*

Assuming the negligible weak link effects and a good grain alignment within the tape, one can use the resistive transitions for a bare core of the tape measured in different fields B in order to deduce the upper critical fields B^i_{C2} and the Ginzburg–Landau coherence lengths ξ_i ($i = a, b$ or c) of the Bi 2223 compound. As illustrated in Fig. 2, both for B perpendicular to the broad surface of the tape (hence approximately parallel to the c-axis of the grains, $B||c$) and for B in the plane of the tape ($B \perp c$), on increasing B, the resistive transitions are broadened, the broadening being the largest at the resistive onset. Although there is no general agreement on the origin of this inhomogeneous broadening of the resistive transitions in HTS [23], we note that at higher resistances, the transitions shift linearly with B as in conventional type II superconductors. Therefore, by adopting a criterion for B_{C2}, one can use these parts of the curves in order to determine $B_{C2}(T)$. The variations of B^c_{C2} and B^{ab}_{C2} (defined by $\rho(T)/\rho_n(T) = 0.5$, where $\rho_n(T)$ is the extrapolated normal state resistivity [12]) with T for our tape are shown in the inset to Fig. 2. The corresponding $B^i_{C2}(0) = T_c(\mathrm{d}B/\mathrm{d}T)$ and $\xi(0)$ values [12] are listed in Table 1. Our values for B^i_{C2}'s in Bi 2223 compound agree quite well with those from the literature [24]. Accordingly our anisotropy ratio $\gamma = \xi_{ab}/\xi_c \approx 5$ agrees with that (≈ 6) from the literature [24], and is also consistent with the anisotropy (4–10) de-

duced from the flux–transformer type of measurements on similar tapes [20]. Our values for B^c_{C2} and ξ_{ab} also agree well with those for Bi 2223 whisker [12], whereas B^{ab}_{C2} for whisker is about six times larger than our value (Table 1). Accordingly, the estimated $\gamma \approx 31$ for Bi 2223 whisker [12] is several times larger that those for well prepared tapes.

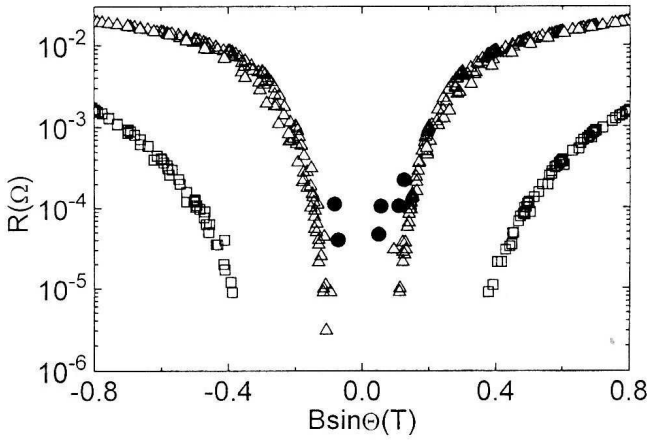

Fig. 3. Plot of resistance versus magnetic field component $B\sin\Theta$ (perpendicular to the plane of the tape) for the sample described in Fig. 2, at temperatures $T = 85$ K(□) and 95 K (△). (●) denotes data for $\Theta \leq 10$ at 95 K.

The above discrepancy may arise due to imperfect grain alignment within the tape. In particular, as evidenced from the X-ray diffraction patterns, the c-axes of the grains show some tilt around the normal to the plane of the tape [13]. From the expression for the angular variation of B_{C2} (derived from the anisotropic Ginzburg–Landau theory [24]), $B_{C2}(\Theta) = B^c_{C2}(\cos^2\Theta + \gamma^{-2}\sin^2\Theta)^{-0.5}$, it is clear that for large γ and small angle Θ, $B_{C2}(\Theta)$ is rather insensitive of Θ, hence $B_{C2}(\Theta) \approx B^c_{C2}$. Therefore, assuming that our B^c_{C2} and $\gamma = 31$ [12] are correct, we can calculate the tilt angle ϕ of the c-axes of the grains within our tape by using our result for $B^{ab}_{C2} = B_{C2}(\pi/2-\phi)$ and the Ginzburg–Landau expression for $B_{C2}(\phi)$. We obtained $\phi \approx 11°$, that compares well with the values of ϕ deduced from the critical current anisotropy in similar tapes [25].

The determination of γ from the ratio of B^i_{C2}'s is not very reliable, because it uses two angles ($B||c$ and $B \perp c$) and limited amount of data from the resistive transitions ($\rho_n(T)/2$) only. Moreover, even in the case of perfect grain alignment, an uncertainty in the actual field direction of 1° would result in the residual (artificial) anisotropy $\gamma = 57$. Because of this, the application of the scalling approach [26] seems more reliable method for the determination of γ. This approach proposes that in an anisotropic superconductor, resistivity scales with the reduced field $B_r = B(\sin^2\Theta + \gamma^2\cos^2\Theta)^{0.5}$, where B is the field magnitude and Θ is the angle between B and the $a-b$ plane. Accordingly, if $\gamma \to \infty$ (2D-scaling), all $\rho(B,\Theta)$ data for a given temperature should fall on the same curve when plotted versus $B_r = B\sin\Theta$.

As illustrated in Fig. 3, $\rho(B, \Theta)$ for the core of our tape seems to obey (within the scatter of the data) 2D-scaling at 85 K, but shows some deviation (filled circles) at 98 K. Since the data points which deviate from the universal curve at 95 K are those for $\theta \leq 10°$, this deviation is clearly due to the misalignment of the grains ($\phi \approx 11°$) within the tape. Clearly, the approximate 2D-scaling for $\Theta \geq 10°$ implies rather large γ but the scatter in the data points (inherent to the measurements of small resistances under very different experimental conditions (Θ, B) over long time intervals) prevents the accurate determination of γ. Because of this we observed the unambiguous deterioration of the scaling behaviour only when assuming $\gamma \leq 10$. Therefore, the results shown in Fig. 3 can only yield an estimate for the lower limit of $\gamma > 10$. Later measurements performed for large angles Θ only indicated $\gamma \geq 30$ which is close to the result for a Bi 2223 whisker [12]. Therefore, our estimate of B_{C2}^{ab} (Table 1) is probably some six times lower than the actual value.

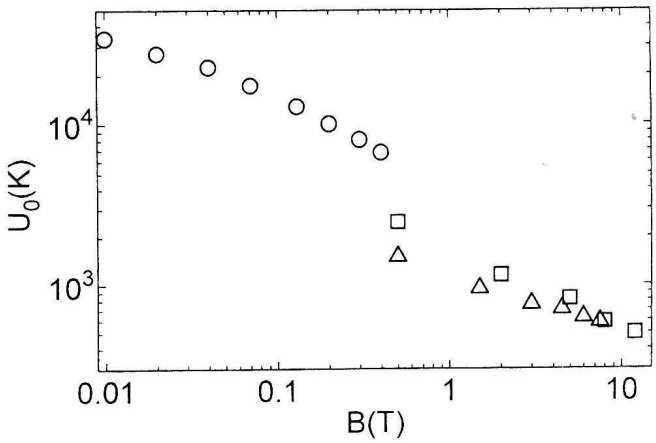

Fig. 4. Pinning potentials U_0 for the core of Bi 2223 *tape (○), epitaxial* Bi 2223 *film (□, Ref. [6]) and* Bi 2223 *whisker (△, Ref. [12]) versus field (parallel to the crystalline c-axis).*

As discussed in some detail elsewhere, both the intact Bi 2223 tape [22] and its bare core [18] show for $J \ll J_c$ an initial resistance variation $R(T, B) \sim \exp(-U/kT)$, where U is an apparent activation energy and k is the Boltzmann constant. For Bi 2223 tapes as well as for the corresponding epitaxial films [6,15] and whisker [12], $U(T, B) = U_0(1 - T/T_c)/B^{\alpha}$ with $\alpha \approx 0.5$, which could be ascribed to the plastic deformation of a flux line solid creating the double kinks, and also to the entanglement of the flux lines in the viscous flux liquid [27]. As mentioned before, there are also other interpretations of the resistive transitions in HTS [23]. However, if the resistive onset is associated with the pinning of the flux lines, then the pinning potential $U_0 = U(T = 0, B)$ should depend on the strength and density of the pinning centres, what depends on the actual method of preparation of the samples of the same compound. As shown in Fig. 4, at lower fields U_0 in Bi 2223 samples increases systematically in order a whisker [12], thin film [6] and

tape [18,22]. (In Fig. 4 we multiplied the measured U_0 of film [6] with the ratio between T_c of the tape and that of the film in order to account for the difference in their T_c's.) Since the density of defects such as the dislocations and stacking faults probably increases in the same order [13], Fig. 4 seems to support the interpretation of the resistive onsets in Bi 2223 samples in terms of the thermally assisted flux motion [18].

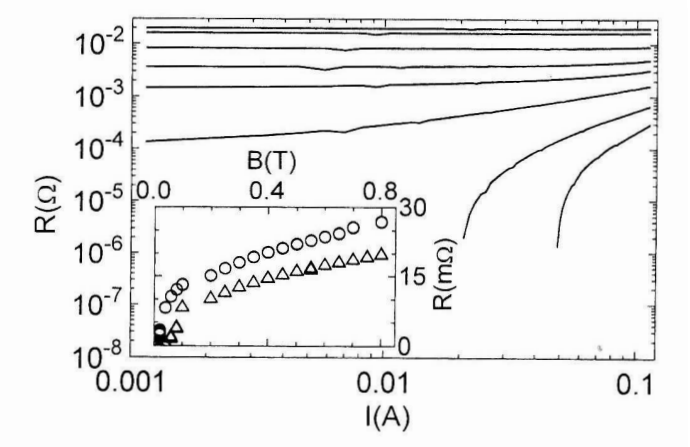

Fig. 5. Plot of resistance vs. current for the bare core of Ag-Bi 2223 *tape at* $T = 100$ K *for fields* B *(parallel to c-axis)* $= 0.01,\ 0.02,\ 0.04,\ 0.06,\ 0.08,\ 0.1,\ 0.5$ and 0.8 T *(bottom to top). The inset: plot of the Ohmic resistance vs. field* B *for a bare core of the* Bi 2223 *tape at* $T = 100$ K *(△) and* 103 K *(○). Note the flux–flow at higher* B.

The observation of the flux–flow resistance R_f is an evidence for the effects of flux motion. Since flux–flow requires high driving force (hence high J and B), these measurements are complicated for HTS (small samples, high J_c and B_{C2}). Because of this, the only detailed measurements of R_f in HTS have so far been performed on $YBa_2Cu_3O_{7-x}$ thin films at temperatures close to T_c [28]. As illustrated in Fig. 5, the variation of the resistance for the bare core of our tape with current, at 100 K, is qualitatively the same as that of $YBa_2Cu_3O_{7-x}$ films around 80 K [28]. As shown in the inset to Fig. 5, both at 100 and 103 K, for $B \geq 0.4$ T, R becomes proportional to B as is expected for R_f [28]. From the slope in the plot of R_f vs. B, one can estimate the flux–flow viscosity coefficient $\eta \approx 10^{-7}$ p for Bi 2223 compound. As for Bi 2212 single crystals [29], this value of η is lower than the Bardeen–Stephen one, $\eta = \phi_0 B^c_{C2}(0)/\rho_n$, estimated from the data in Table 1. The reason for this difference (in addition to that put forward for Bi 2212 single crystals [29]) may be the enhanced increase of R_f with B in the vicinity of T_c [24]. The data in the inset to Fig. 5 seem to support this conjecture.

Finally, we consider the nature of the flux pinning in Bi 2223 tapes. For this purpose, in addition to U_0, we use the variation of J_c with B measured on the same tape. As reported earlier [17,18,22], for $T \geq 77$ K, J_c of the single phase Bi 2223

tapes shows a $(1-T/T_c)^{1.5}$ and initial $B^{-0.5}$ variations with T and B, respectively. These variations are reminiscent of the flux–creep and contrast sharply with the weak–link dominated variations of J_c with T and B in ceramic samples [11].

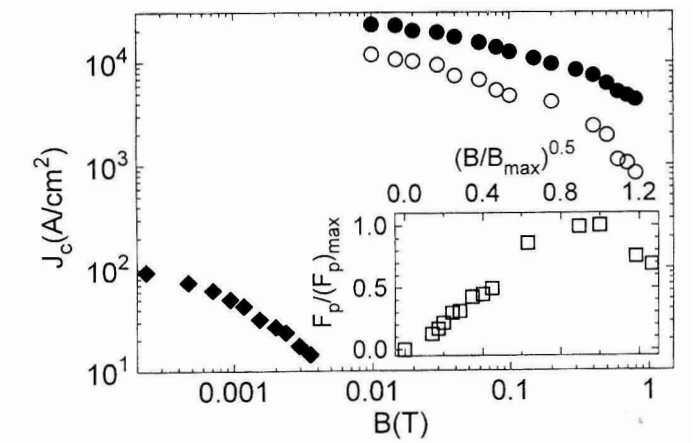

Fig. 6. Plot of the critical current density vs. field B, at T = 81 K, for the ceramic Bi 2223 *sample S_A (◇) and* Bi 2223 *tape (● and ○ for B parallel and perpendicular to the plane of the tape, respectively). The inset: plot of volume pinning force $F_p = J_cB$, normalized to its maximum value vs. normalized field showing a $F_p \sim B^{0.5}$ variation in* Bi 2223 *tape.*

As seen from Table 1 and illustrated in Fig. 6, for T = 81 K, $J_c(B = 0)$ for ceramic sample S_A is over two orders of magnitude lower than that of our tape. Furthermore, in S_A, J_c decreases ten times in a field of a few mT, whereas for the tape, a field of about 1 T is required for a similar suppression of J_c. As shown in Fig. 6, J_c of the tape decreases faster with B for $B||c$ than for $B \perp c$, whereas in ceramic samples, J_c shows no such anisotropy [11]. The absence of anisotropy in ceramic samples arises from the isotropic percolative current path in these materials. Accordingly, the observed anisotropy of J_c in tapes indicates that the current path, although percolative, is not isotropic in these materials. In particular, current flows along the $a-b$ planes of the well connected grains whose c-axes are approximately perpendicular to the surface of the tape. However, the anisotropy of J_c in epitaxial Bi 2223 films [6,15] is much larger than that in our tape (Fig. 6). Clearly, this difference arises from the imperfect grain alignment along the current path in tapes, which masks a large intrinsic anisotropy of the Bi 2223 compound [12]. Indeed, by assuming that only the component of field $B||c$ affects J_c (2D-scaling [26]), and that the grains whose $a-b$ planes form an angle ϕ with the plane of the tape are symmetrically distributed around $\phi = 0$ within two planes defined with the limiting angles ϕ_0 and $-\phi_0$, one can calculate ϕ_0 from $\sin\phi_0 = B_1/B_2$, where $B_1||c$ and $B_2 \perp c$ are fields corresponding to the same value of J_c [25]. From $J_c - B$ variations for our tape (Fig. 6), we found $\phi_0 = 8 \pm 2°$, which is quite close to the estimates for ϕ obtained from the resistive transitions. Furthermore, ϕ_0 was insensitive of B, which indicates the absence of weak links

along the current path.

Although reminiscent of the flux–creep, the initial rapid decrease of $J_c \sim B^{-0.5}$ is often attributed to the intergranular weak links [20]. In our opinion, the observed variations of U_0 and J_c with B provide the selfconsistent description of the nature of pinning in these materials. According to the collective pinning model [30], the dense, randomly distributed pinning centres lead to a glassy array of vortices, in which their positions are correlated only within the flux bundle of volume V_c. The pinning forces within V_c add randomly, hence $F_c \sim U_c \sim V_c^{0.5}$, where F_c is the pinning force on the bundle and U_c is the energy with which the bundle is pinned. Therefore, the pinning force per unit volume, $F_p = F_c/V_c = J_c B$, should be inversely proportional to U_c. As illustrated in the inset to Fig. 6, for our tape at $T = 81$ K and $B||c$, $F_p \sim B^{0.5}$ up to $B_{max} \approx 0.5$ T has been observed. Since within the same T and B range U for our tape varied as $B^{-0.5}$, this result indicates the collective pinning of vortices.

4. Conclusion

The systematic study of the electron transport properties (ρ, J_c) and AC susceptibility performed in the temperature (T) range 77–120 K and magnetic fields (B) up to 1 T, revealed very different behaviours for two types of the almost single phase Pb-doped Bi 2223 polycrystalline samples. Whereas in the conventionally prepared ceramic samples, the weak–links at the intergranular boundaries mask efficiently the intrinsic properties of the Bi 2223 compound, the Ag-clad Bi 2223 tape exhibits the non weak-linked behaviour, which is, for the field perpendicular to the plane of the tape ($B||c$), analogous to that observed in Bi 2223 epitaxial films [6,15] and Pb-doped Bi 2223 whiskers [12]. Accordingly, we used the $V-I$ curves and the magnetoresistance of our tape (measured for $B||c$) in order to deduce B_{C2}^c, ξ_{ab} and the flux–flow viscosity η for the Bi 2223 compound. The results for B_{C2} and ξ_{ab} (Table 1) agree with those obtained from the measurements on the corresponding whiskers [12]. Our observation of the flux–flow is the first one for Bi 2223 samples and proves the contribution of the flux motion in the broadening of the resistive transition in this compound. For the other field directions (including $B \perp c$), our results deviate somewhat from those for the epitaxial films and whisker. This can be explained in terms of the percolative current path along the tape, involving the grains which form a tilt angle ϕ with the ribbon axis. All our measurements are consistent with the maximum tilt angle $\phi_0 = 10 \pm 2°$. After the correction for ϕ_o, our results for the other field directions become consistent with those for whiskers.

The broadening of the resistive transition with field for tape is smaller than that observed in the corresponding films and whisker. Accordingly, the pinning potential U_0 is larger but it shows the same variation $U_0 \sim B^{-0.5}$ as in other types of Bi 2223 samples. This variation of U_0 taken together with the observed $F_p \sim B^{0.5}$ variation of the volume pinning force ($F_p = J_c B$) shows that the pinning of vortices in Bi 2223 tapes is collective [30]. The enhanced pinning of vortices in Bi 2223 tapes with respect to those in Bi 2223 films and whiskers, can be associated with the abundancy of defects within the grains of the tapes [13].

In spite of the enhanced pinning, the highest J_c in the present-day tapes is

up to ten times lower than that in the best epitaxial films [6,15]. This implies a percolative current path along a rather low fraction of well connected grains within the tape. Accordingly the local current density J_{cl} along this path is probably several times larger than the overall J_c. Indeed, large variations of J_c, both along the width [18] and length of the Bi 2223 tapes, have been observed. Therefore, a more dense and homogeneous tapes should exhibit higher J_c. A denser core of the tape can be obtained from the more dense packing of the calcined powder within the Ag-tube. This can be achieved by using the mixture containing two or more different sizes of the grains [31]. The grain alignment and the homogeneity of the core depend on the mechanical work performed on the tape [13]. We suggest that by replacing the usual rolling + pressing routine with rolling with the deformable rollers can yield more homogeneous tapes. The high field performance of the present day tapes can be improved inexpensively by using the splayed defects arising from the nuclear fission of the suitable material incorporated either within the core or in the Ag-sheating. Clearly, there is ample space for the further improvement of the current-carrying properties of the Ag-clad Bi 2223 and Bi 2212 tapes.

Acknowledgement

We thank N.I.S.T. (USA), Metal Manufacturers (Australia), Commonwealth Department of Industry, Technology and Commerce and Australian Research Council for the financial support.

References

1) H. Maeda, Y. Tanaka, M. Fukutomi and T. Asano, Jpn. J. Appl. Phys. **27** (1988) L209;

2) S. Bernik, M. Horvat and D. Kolar, Supercond. Sci. Technol. **7** (1994) 920;

3) D. Đurek, Z. Medunić, V. Manojlović, M. Prester, E. Babić, K. Zadro, B. Rakvin and M. Požek, Modern Phys. Lett. **B3** (1989) 1135;

4) D. Shi, M. Tang, K. Vandervoort and H. Claus, Phys. Rev. B **39** (1989) 9091;

5) Y. Hakuraku, D. Miyagi, S. Higo and T. Ogushi, Jpn. J. Appl. Phys. **29** (1990) L926;

6) H. Yamasaki, K. Endo, S. Kosaka, M. Umeda, S. Yoshida and K. Kajimura, Phys. Rev. Lett. **70** (1993) 3331 and refs. therein;

7) K. Aota, H. Hatori, T. Hatano, K. Nakamura and K. Ogawa, Jpn. J. Appl. Phys. **28** (1989) L2196;

8) S. L. Lin, C. Tien, T. S. Chin, T. W. Huang and M. P. Hung, Jpn. J. Appl. Phys. **29** (1990) L775;

9) G. Miehe, T. Vogt, H. Fuess and M. Wilhelm, Physica **C171** (1990) 339;

10) P. Bordet, J. J. Caponi, C. Chaillout, J. Chenavas, A. W. Hewat, E. A. Hewat, J. L. Hodeau and M. Marezio, in *Studies of High Temperature Superconductors*, ed. A. Narlikar, Nova Science Publishers, New York (1989) vol.2 p.171;

11) E. Babić, M. Prester, D. Babić, Ž. Marohnić and Đ. Drobac, Fizika A **1** (1992) 67;

12) I. Matsubara, H. Tanigawa, T. Ogura, H. Yamashita, M. Kinoshita and T. Kawai, Phys. Rev. **45** (1992) 7414 and refs. therein;

13) S. X. Dou and H. K. Liu, Supercond. Sci. Technol. **6** (1993) 197;

14) T. T. M. Palstra, R. Batlogg, L. F. Schneemeyer and J. W. Waszczak, Phys. Rev. B **43** (1991) 3756;

15) P. Wagner, F. Hilmer, U. Frey, A. Hadish, Th. Becherer, E. Eckert, T. Steinborn, J. Wiesner, G. Wirth and H. Adrian, in Proceedings of 7th International Workshop on Critical Currents in Superconductors, Ed. H. W. Weber, World Scientific (1994) p. 82;

16) Q. Li, M. Suenaga, J. Gohng, D. K. Finnemore, T. Hikata and K. Sato, Phys. Rev. B **46** (1992) 3195;

17) I. Kušević, Ž. Marohnić, E. Babić, J. Ivkov, M. Prester, H. K. Liu, Q. Y. Hu and S. X. Dou, in Proceedings of 7th International Workshop on Critical Currents in Superconductors, Ed. H. W. Weber, World Scientific (1994) p. 557;

18) I. Kušević, E. Babić, J. Ivkov, Ž. Marohnić, H. K. Liu, Q. Y. Hy and S. X. Dou, Solid State Commun. **92** (1994) 735;

19) Ž. Marohnić, Đ. Drobac, E. Babić, H. K. Liu and S. X. Dou, J. of Superconductivity **7** (1994) 809;

20) J. H. Cho, M. P. Maley, J. O. Willis, J. Y. Coulter, L. N. Bulaevskii, P. Haldar and R. L. Motowidlo, Appl. Phys. Lett. **64** (1994) 3030;

21) M. Prester, E. Babić, M. Stubičar and P. Nozar, Phys. Rev. B **49** (1994) 6967;

22) E. Babić, I. Kušević, S. X. Dou, H. K. Liu and Q. Y. Hu, Phys. Rev. B **49** (1994) 15312;

23) K. Kadowaki, Y. Songliu and K. Kitazawa, Supercond. Sci. Technol. **7** (1994) 519;

24) M. Cyrot and D. Pavuna, *Introduction to Superconductivity and High-T_c Materials* (World Scientific, Singapore, 1992) p. 181;

25) Q. Y. Hu, H. W. Weber, S. X. Dou, H. K. Liu and H. W. Neumiller, J. of Alloys and Compounds **195** (1993) 515;

26) G. Blatter, V. B. Geshkenbein and A. I. Larkin, Phys. Rev. Lett. **68** (1992) 895;

27) V. M. Vinokur, M. V. Feigel'man, V. B. Geshkenbein and A. I. Larkin, Phys. Rev. Lett. **65** (1990) 259 and refs. therein;

28) M. N. Kunchur, D. K. Christen and J. M. Phillips, Phys. Rev. Lett. **70** (1993) 998;

29) L. N. Bulaevskii, J. H. Cho, M. P. Maley, P. Kes, Qiang Li, M. Suenaga and M. Ledvij, Phys. Rev. B **50** (1994) 3507;

30) A. I. Larkin and Yu. N. Ovchinnikov, J. of Low Temperature Physics **34** (1979) 409;

31) J. M. Ziman, *Models of Disorder* (Cambridge Univ.Press, 1979) p. 98.

SUPRAVODLJIVOST U SPOJU Bi 2223: FIZIKA I MOGUĆE PRIMJENE

Prikazani su glavni rezultati sustavnog istraživanja električnih svojstava i inicijalne susceptibilnosti gotovo–monofaznih Bi 2223 keramičkih uzoraka dopiranih olovom i srebrom obložene vrpce. Dok se rezultati za keramičke uzorke mogu primjenjivati isključivo za proučavanje perkolacije u sustavu slabih veza, oni za traku daju neke intrinsične parametre Bi 2223 spoja (viša kritična polja i duljine koherencije). Nadalje, rezultati za traku daju neke tehnološki važne parametre (potencijal zapinjanja U_0, volumnu gustoću sile zapinjanja F_p i viskoznost tečenja magnetskih vrtloga η) i uvid u prirodu rasipanja energije i zapinjanja vrtloga u tim materijalima. Ukratko su razmotreni razlozi ograničenja kritičnih struja u vrpcama.